

Electronic Supplementary Information

Metronidazole-functionalized iron oxide nanoparticles for molecular targeting of hypoxic tissue

Miriam Filippi,^{1,2} Dinh-Vu Nguyen,³ Francesca Garello,⁴ Francis Perton,³ Sylvie Bégin-Colin,³ Delphine Felder-Flesch,³ Laura Power,^{1,2} and Arnaud Scherberich^{1,2}*

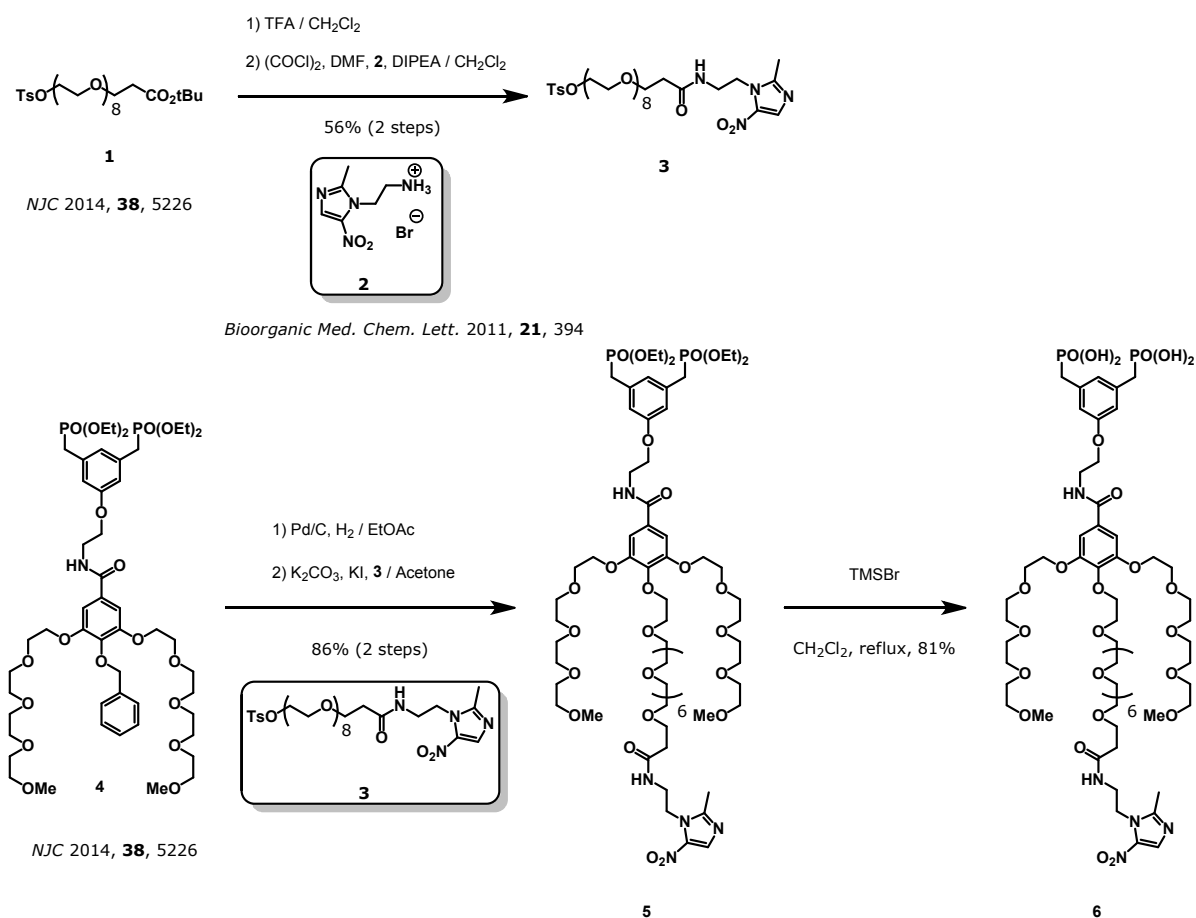
¹Department of Biomedical Engineering, University of Basel, Gewerbestrasse 14, 4123, Allschwil, Basel, Switzerland

²Department of Biomedicine, University Hospital Basel, University of Basel, Hebelstrasse 20, 4031, Basel, Switzerland

³Université de Strasbourg, CNRS, Institut de Physique et Chimie des Matériaux de Strasbourg, UMR 7504, F-67000 Strasbourg, France

⁴Molecular and Preclinical Imaging Centers, Department of Molecular Biotechnology and Health Sciences, University of Torino, Torino, Italy.

1. Synthesis of ligands: Metro-dendron



Scheme S1. Complete scheme of the synthetic procedure to generate metro-dendrons.

The complete synthetic procedure to generate metro-dendrons is represented, also showing the insertion of the targeting vector metronidazole by functionalization of the phenolic group on the compound **4**, before the deprotection final step of the phosphonate anchoring sites on the compound **5**.

1.1 Synthetic Procedure

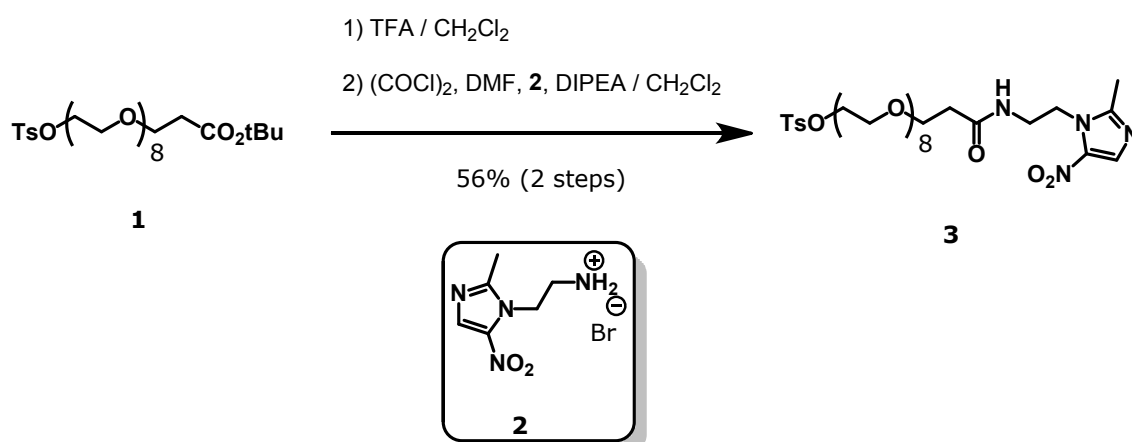
1.1.1 Generation of the intermediate compound 3.

A solution of compound **1**¹ (1347.4 mg, 2.1 mmol) in CH₂Cl₂ (20 mL) had TFA (1.3 mL, 16.5 mmol, 8.0 equiv.) added to it at RT. The resulting solution was stirred at RT for 16 h, then concentrated under reduced pressure. Next, crude carboxylic acid was dissolved in CH₂Cl₂, then (COCl)₂ (0.5 mL, 5.9 mmol, 2.8 equiv.) and DMF (4 drops) were added at RT. The solution was stirred at RT for 4 h, then concentrated under reduced pressure. The acyl chloride was next dissolved in CH₂Cl₂, then compound **2**² (529.0 mg, 2.1 mmol, 1.02 equiv.) and DIPEA (5.0 mL, 28.7 mmol, 13.7 equiv.) were added at RT. The resulting solution was stirred at RT for 16 h, then concentrated under reduced pressure. The crude residue was purified by reverse phase C₁₈ chromatography (CH₃CN/H₂O + 1% TFA 3/7 to 4/6 to 1/1) to obtain 870 mg (1.16 mmol, 56%) of compound **3**.

Physical state: brown oil.

A. Garofalo, A. Parat, C. Bordeianu, C. Ghobril, Ma. Kueny-Stotz, A. Walter, J. Jouhannaud, S. Begin-Colin, D. Felder-Flesch, *New J. Chem.* **2014**, 5226–5239.

² J. Giglio, S. Fernández, A. Rey, H. Cerecetto, *Bioorganic Med. Chem. Lett.* **2011**, 21, 394–397.



Scheme S2. Generation of intermediate compound 3. The synthetic procedure to generate the compound **3** by reaction of compound **1** with compound **2** is represented.

1.1.2 Characterization of intermediate compound 3.

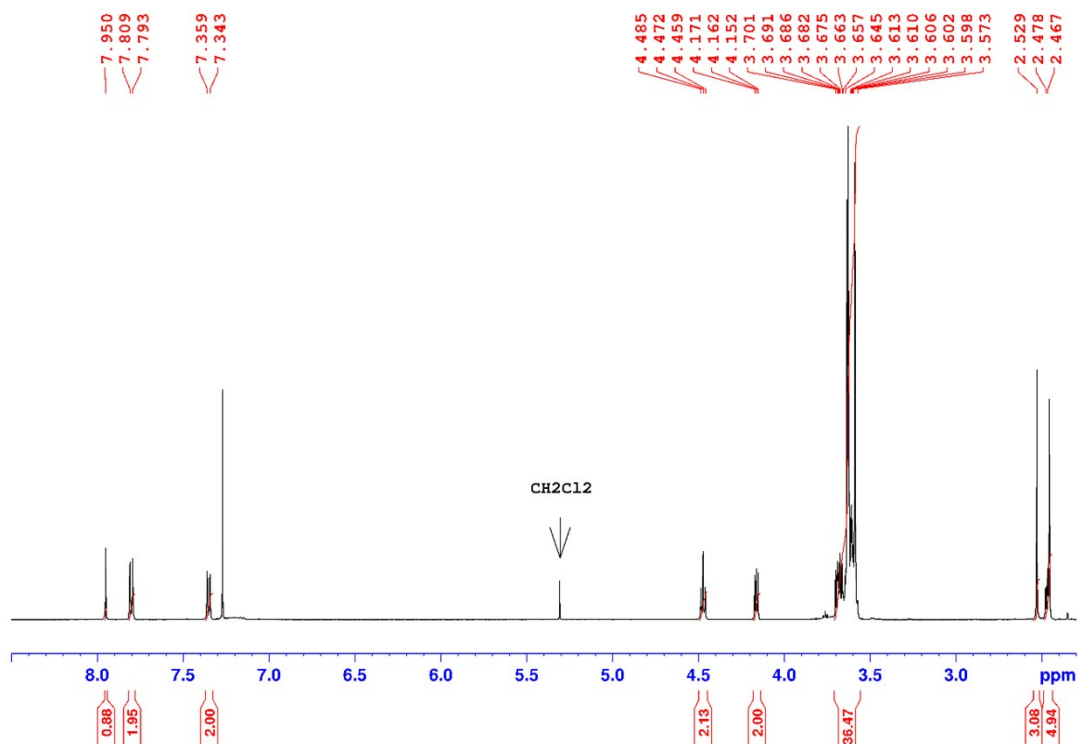


Figure S1. Characterization of intermediate compound 3 by ¹H NMR spectroscopy. After generation the compound 3 was characterized by ¹H NMR spectroscopy, obtaining following results. ¹H NMR (500 MHz, CDCl₃): δ 7.94 (s, 1H), 7.80 (dd, *J* = 8.2, 1.9 Hz, 2H), 7.35 (dd, *J* = 8.0, 2.0 Hz, 2H), 4.47 (t, *J* = 6.2 Hz, 2H), 4.16 (t, *J* = 4.7 Hz, 2H), 3.70—3.57 (m, 36H), 3.07 (s, 3H), 2.46 (t, *J* = 5.5 Hz, 2H), 2.45 (s, 3H) ppm

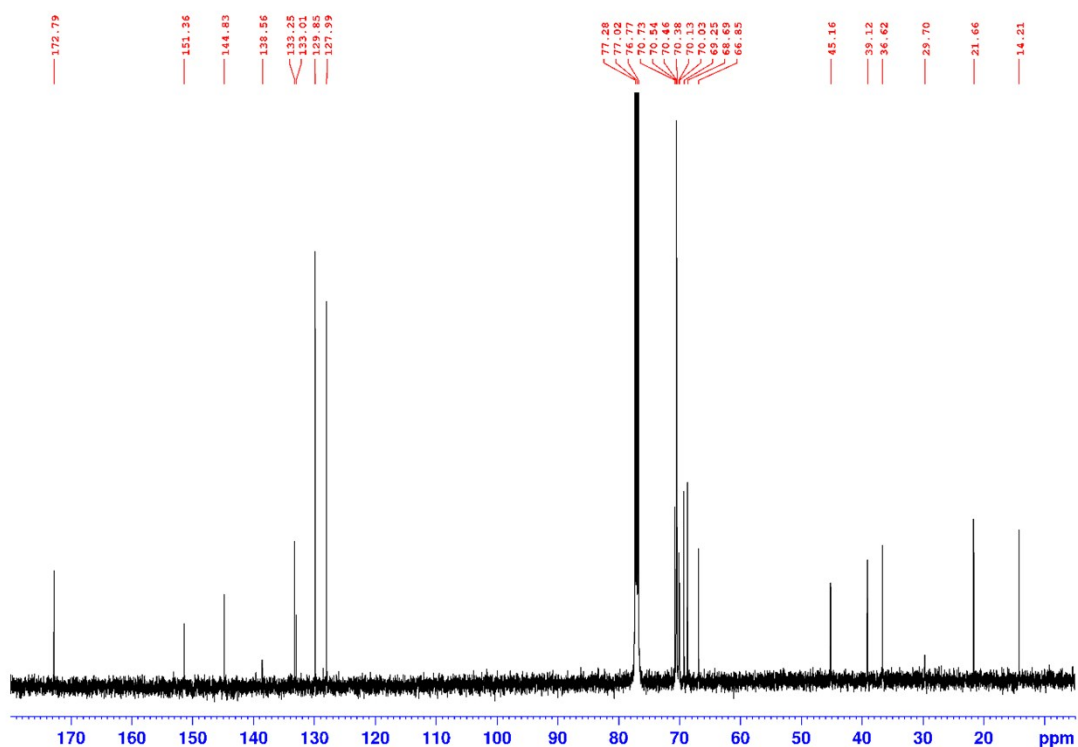


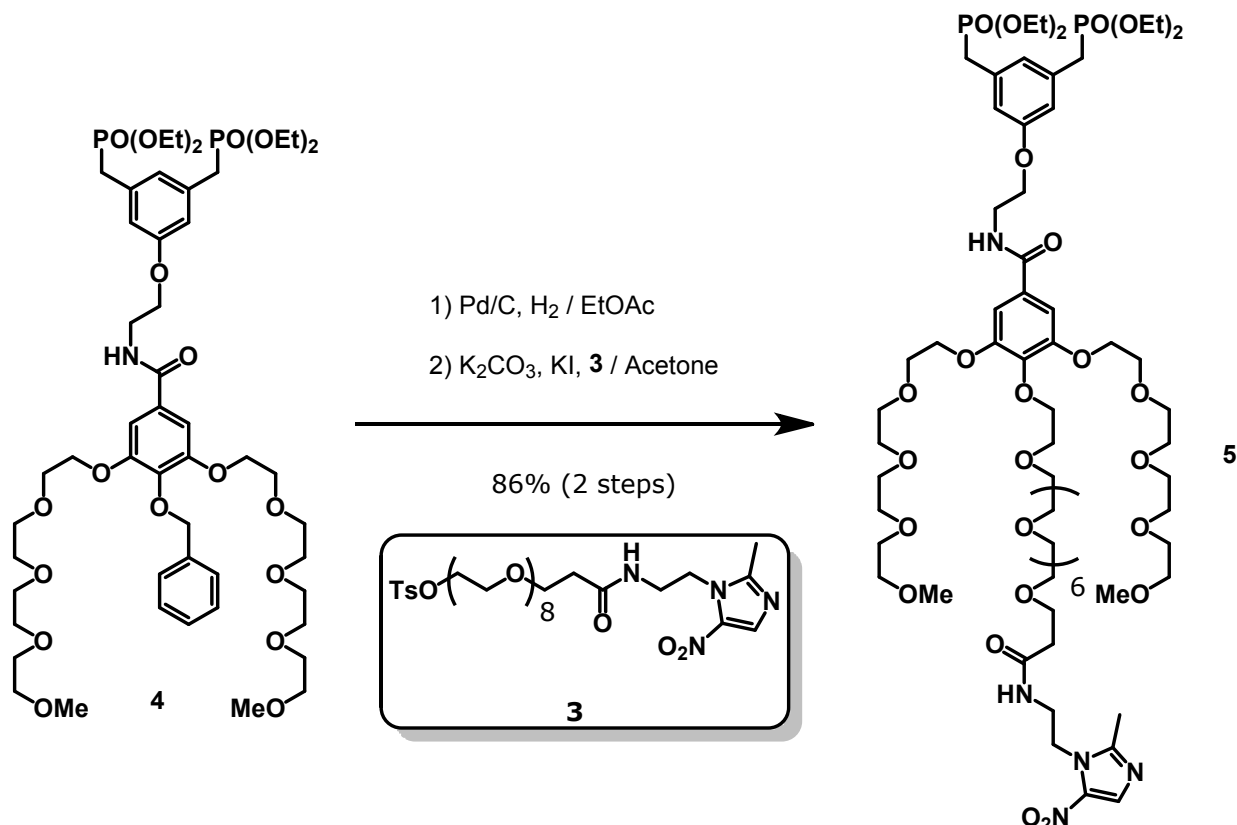
Figure S2. Characterization of intermediate compound 3 by ¹³C NMR spectroscopy. After generation, the compound 3 was characterized by ¹³C NMR spectroscopy, obtaining following results. ¹³C NMR (125 MHz, CDCl₃): δ 172.7, 151.3, 144.8, 138.5, 133.2, 133.07, 129.8, 127.9, 70.7, 70.5, 70.4 (several peaks), 70.3, 70.1, 70.0, 69.2, 68.6, 66.8, 45.1, 39.1, 36.6, 21.6, 14.2 ppm

1.1.3 Generation of intermediate compound 5

A solution of compound 4¹ (161.2 mg, 0.15 mmol) in EtOAc (4 mL) had Pd/C 10% (16.2 mg, 0.02 mmol, 0.1 equiv.) added to it at RT. The heterogeneous solution was evacuated and backfilled with an atmosphere of hydrogen (balloon), vigorously stirred at RT for 16 h, then the catalyst was filtered off over Celite and the crude product was concentrated under reduced pressure. The crude phenol was next dissolved in acetone (4 mL), then compound 3 (119.6 mg, 0.16 mmol, 1.05 equiv.), K₂CO₃ (31.5 mg, 0.23 mmol, 1.5 equiv.), and KI (2.5 mg, 0.02 mmol, 0.1 equiv.) were added. The resulting solution was heated to reflux for 16 h, cooled to RT, then concentrated under reduced pressure. The crude residue was suspended in CH₂Cl₂,

the solids were filtered over Celite, and the crude product was concentrated under reduced pressure. Purification by chromatography on silica gel ($\text{CH}_2\text{Cl}_2/\text{MeOH}$ 96/4 to 92/8 to 84/16) produced 202.3 mg (0.13 mmol, 86%) of compound **5**.

Physical state: orange oil.



Scheme S3. Generation of intermediate compound 5. The synthetic procedure to generate the compound **5** by reaction of compound **4** with compound **3** is represented.

1.1.4 Characterization of intermediate compound 5

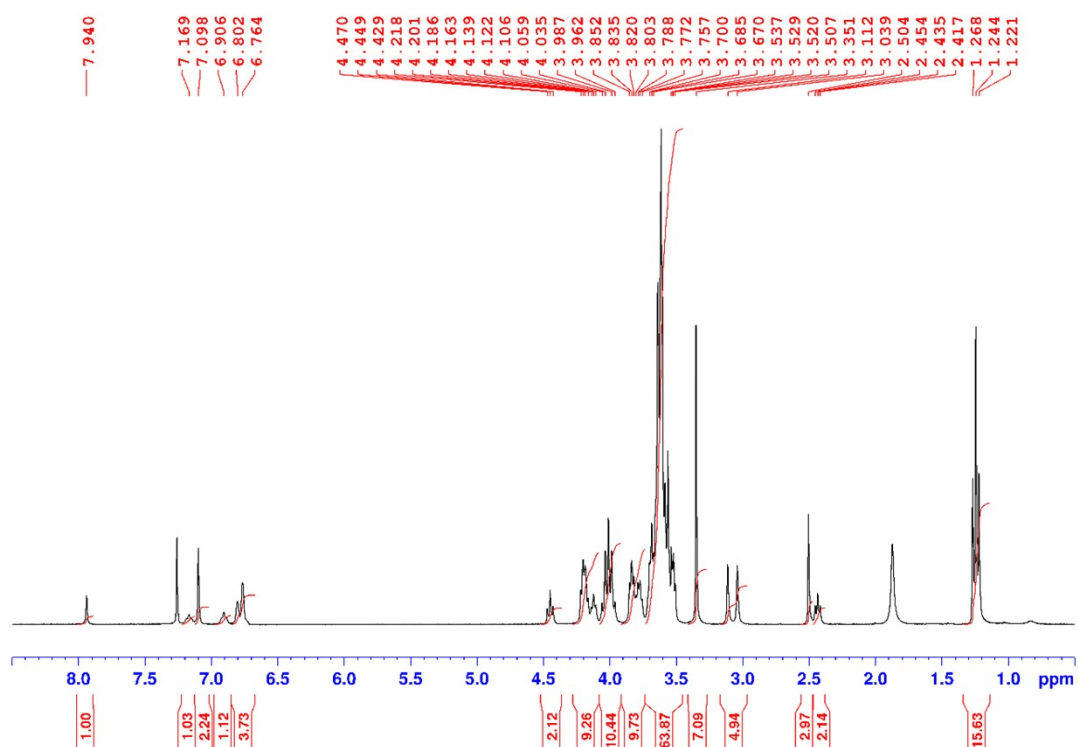


Figure S3. Characterization of intermediate compound 5 by ^1H NMR spectroscopy. After generation the compound 5 was characterized by ^1H NMR spectroscopy, obtaining following results. ^1H NMR (300 MHz, CDCl_3): δ 7.96 (s, 1H), 7.13 (brs, 1H), 7.09 (s, 2H), 6.85 (brs, 1H), 6.80 (s, 1H), 6.76 (s, 2H), 4.45 (t, $J = 6.3$ Hz, 2H), 4.20 (t, $J = 4.8$ Hz, 4H), 4.18 (t, $J = 5.0$ Hz, 2H), 4.12 (t, $J = 5.1$ Hz, 2H), 4.01 (qt, $J = 7.4$ Hz, 8H), 3.83 (t, $J = 4.8$ Hz, 4H), 3.81—3.76 (m, 4H), 3.60—3.51 (m, 61H), 3.35 (s, 6H), 3.07 (d, $^2J_{P-H} = 21.7$ Hz, 4H), 2.50 (s, 3H), 2.43 (t, $J = 5.7$ Hz, 2H), 1.24 (t, $J = 7.3$ Hz, 12H) ppm.

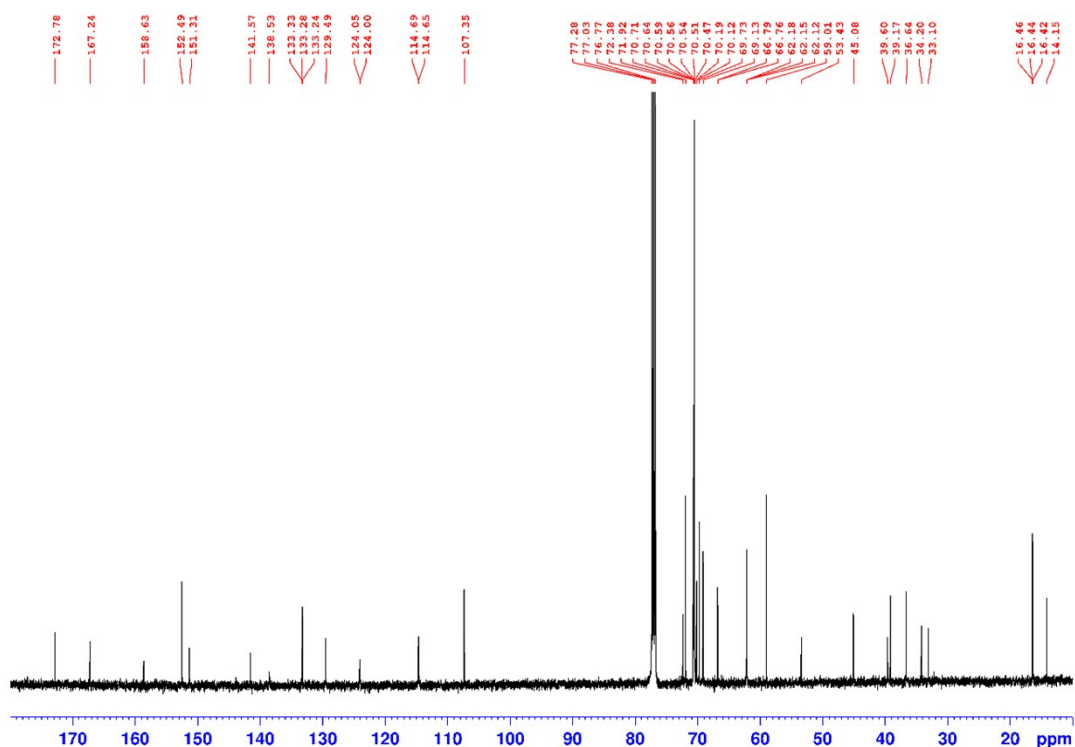


Figure S4. Characterization of intermediate compound 5 by ^{13}C NMR spectroscopy.

After generation, the compound **5** was characterized by ^{13}C NMR spectroscopy, obtaining following results. ^{13}C NMR (125 MHz, CDCl_3): δ 172.7, 167.2, 158.6, 152.4, 151.3, 141.5, 138.5, 133.3 (t, $^2J_{\text{C-P}} = 6.1$ Hz), 133.2, 129.4, 124.0 (t, $^3J_{\text{C-P}} = 6.4$ Hz), 114.6 (t, $^3J_{\text{C-P}} = 4.5$ Hz), 107.3, 72.3, 71.9, 70.7, 70.6, 70.5 (several peaks), 70.4, 70.1, 69.7, 69.1 66.7, 62.1 (d, $^2J_{\text{C-P}} = 7.0$ Hz), 59.0, 45.0, 39.6, 39.1, 36.6, 33.6 (d, $^1J_{\text{C-P}} = 138.6$ Hz), 16.4 (d, $^3J_{\text{C-P}} = 5.7$ Hz), 14.1 ppm.

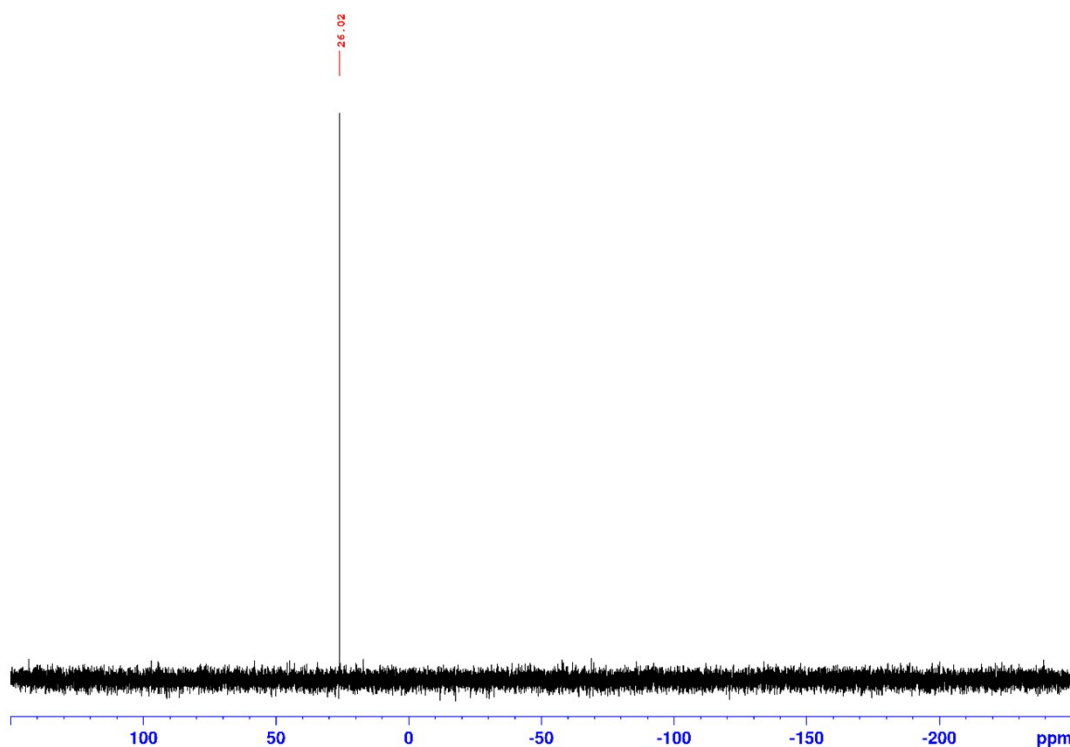
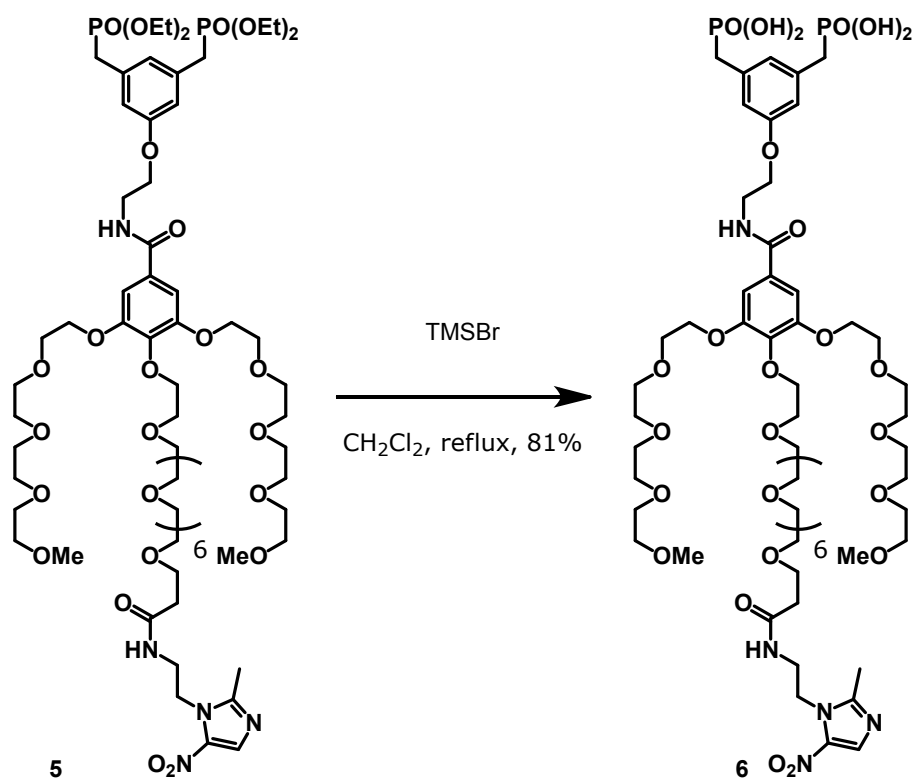


Figure S5. Characterization of intermediate compound 5 by ^{31}P NMR spectroscopy. After generation, the compound 5 was characterized by ^{31}P NMR spectroscopy, obtaining following results. ^{31}P NMR (121 MHz, CDCl_3): δ 26.0 ppm.

1.1.5 Generation of intermediate compound 6

A solution of compound 5 (150.7 mg, 0.1 mmol) in CH_2Cl_2 (2 mL) had TMSBr (0.2 mL, 1.5 mmol, 15.0 equiv.) added to it at RT. The resulting solution was heated to reflux for 2 h, cooled to RT, and quenched with MeOH. The crude product was concentrated under reduced pressure, then purified by LH20, eluted with MeOH to produce 113.7 mg (0.08 mmol, 81%) of compound 6.

Physical state: yellow gum.



Scheme S4. Generation of compound 6. The synthetic procedure to generate the compound **6** by deprotection of compound **5** is represented.

1.1.4 Characterization of intermediate compound 6

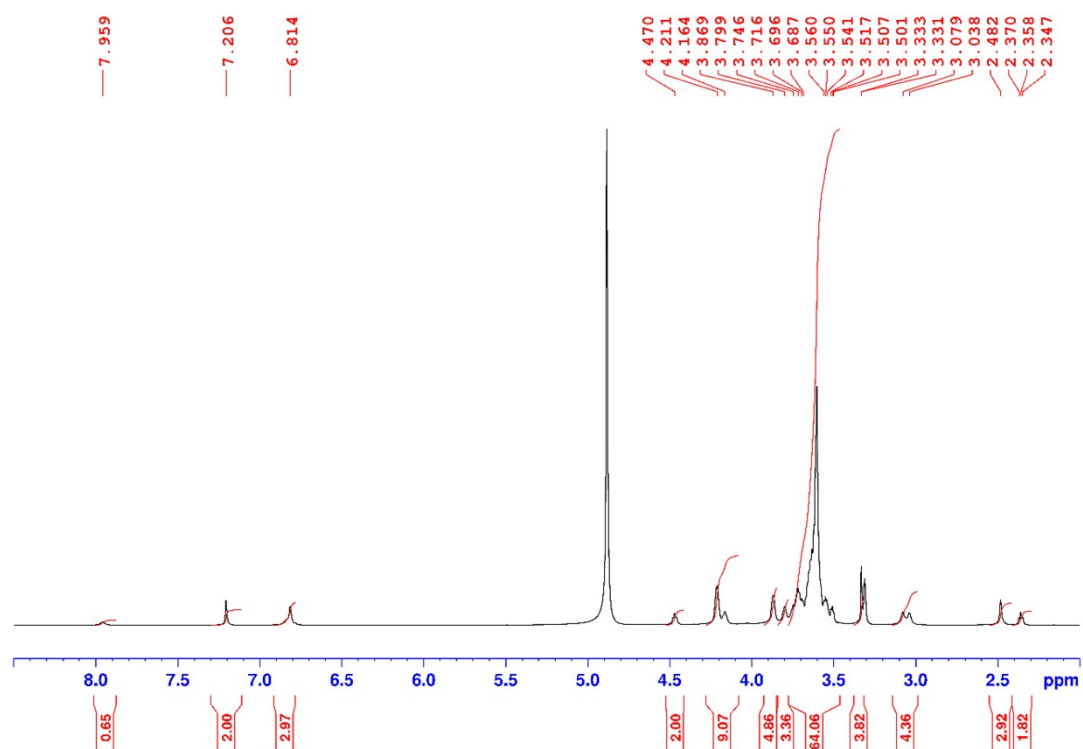


Figure S6.

¹H NMR (500 MHz, CD₃OD-*d*₄): δ 7.95 (s, 1H), 7.20 (s, 2H), 6.84 (s, 1H), 6.81 (s, 2H), 4.46 (t, *J* = 6.1 Hz, 2H), 4.23—4.19 (m, 6H), 4.16 (t, *J* = 5.8 Hz, 2H), 3.86 (t, *J* = 4.7 Hz, 4H), 3.79 (t, *J* = 4.7 Hz, 2H), 3.76—3.50 (m, 64H), 3.30 (s, 3H), 3.05 (d, ²*J*_{P-H} = 20.2 Hz, 4H), 2.48 (s, 3H), 2.35 (t, *J* = 5.0 Hz, 2H) ppm

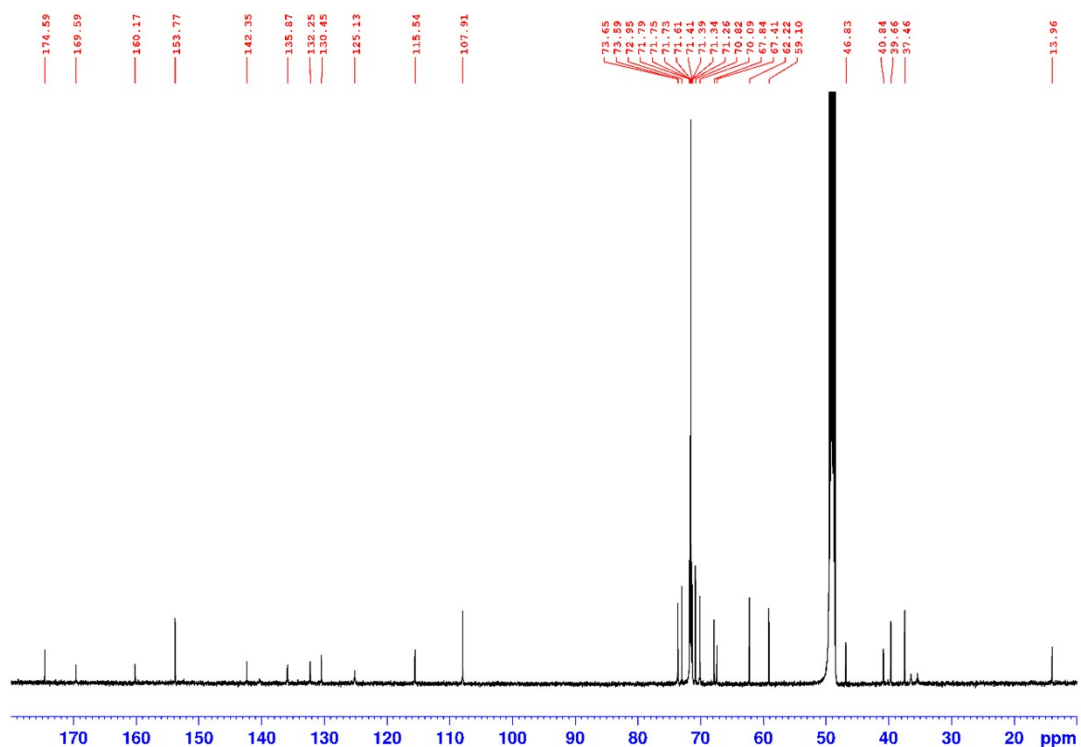


Figure S7.

^{13}C NMR (125 MHz, $\text{CD}_3\text{OD}-d_4$): δ 174.5, 169.5, 160.1, 153.7, 142.3, 135.8, 132.2, 130.4, 125.1, 115.5, 107.9, 73.6, 73.5, 72.9, 71.7—71.5 (several peaks), 71.4, 71.3, 71.2, 70.8, 70.0, 67.8, 67.4, 62.2, 59.1, 46.8, 40.8, 39.6, 37.4, 36.0 (d, $^1J_{C-P} = 32.9$ Hz), 13.9 ppm

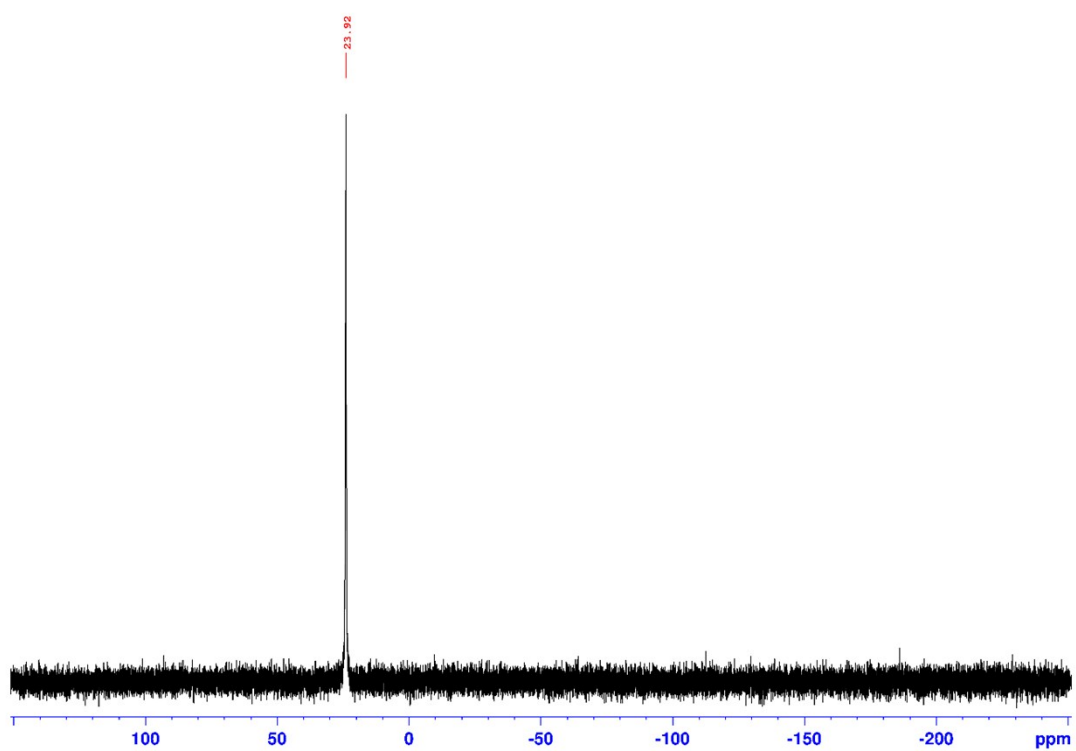


Figure S8.

^{31}P NMR (202 MHz, $\text{CD}_3\text{OD}-d_4$): δ 23.9 ppm

2. Synthesis, functionalization, and characterization of nanoparticles

2.1 Synthesis of spherical nanoparticles of 10 nm

In a 100 mL two-necked flask, iron II stearate (2.2 mmol, 1.38 g), oleic acid (4.4 mmol, 1.24 g), and dioctyl ether (20 mL) were mixed together. The resulting solution was heated at 120°C for 1 h under magnetic stirring without reflux condenser. Following this step, the magnetic stirrer was removed and the condenser connected to the flask. The solution was heated up to 298°C for 2 h at a heating rate of 5°C/min. After cooling, a black suspension was collected and precipitated by the addition of acetone. Finally, the particles were washed three times with a mixture 1:4 chloroform:acetone.

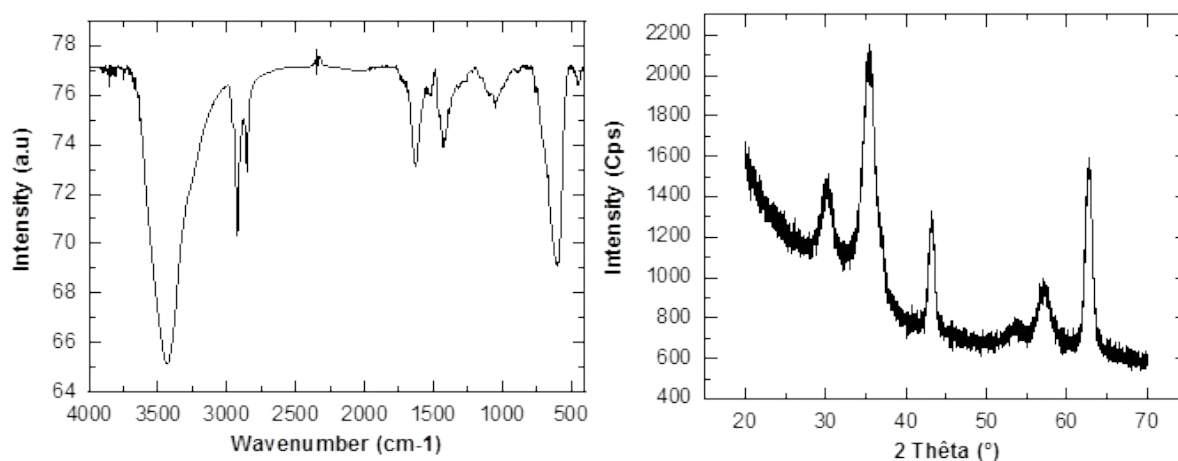


Figure S9. Characterization of NPs. Fourier transform infrared (FTIR) (left) and X-ray diffraction spectra (right) of the uncoated spherical 10 nm iron oxide nanoparticles.

2.2 Functionalization of nanoparticles

In a 30 mL glass vial, a nanoparticle suspension in THF (5 mg of iron) was combined with compound **6** (5.25 mg). The vial was completed with 25 mL of THF. The mixture was magnetically stirred for 30 min, and then compound **7** (1.75 mg) was added to the reaction mixture and stirred for 24 h. The resulting particles were centrifuged and added with cyclohexane, dispersed in water, and washed by ultrafiltration.

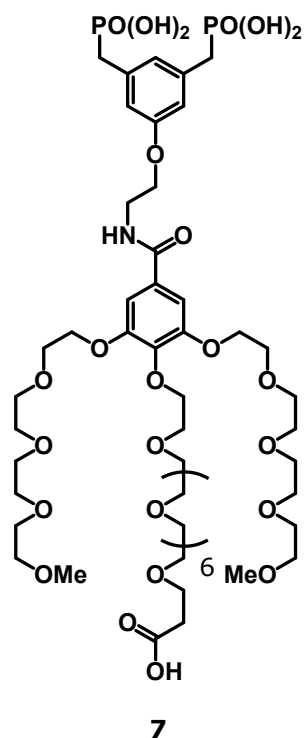


Figure S10. Structure of compound 7. Schematic representation of the structure of the compound 7 used to functionalize nanoparticles.

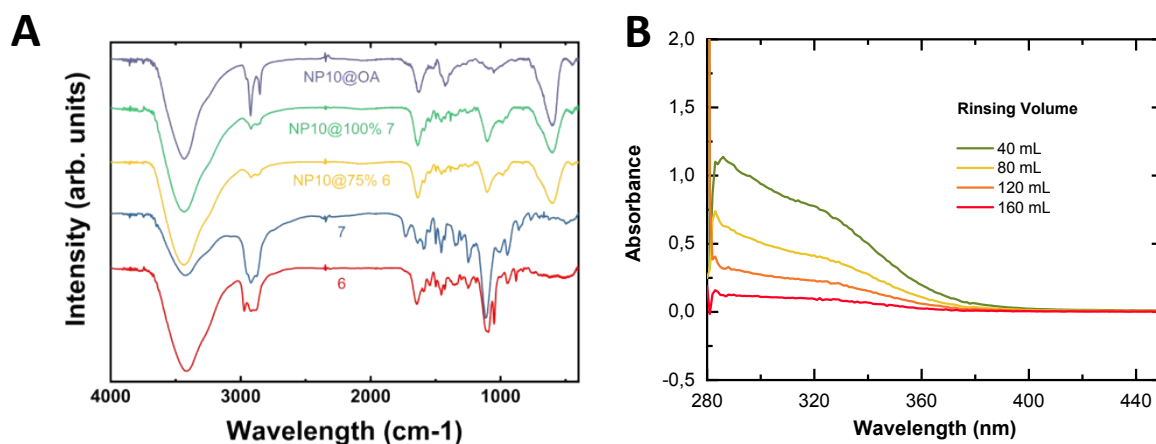


Figure S11. Characterization of functionalized NPs. Variation of the FTIR spectrum of nanoparticles as a function of the ligand on the surface (left): oleic acid (OA)-coated iron oxide nanoparticles (OA-NPs, blue line), NPs coated with the phosphonated dendron (NPs@7, green line), or with metro-functionalized dendrons (metro 75%-NPs, orange line), phosphonated dendrons (compound 7, blue line), and metro-functionalized-dendrons (compound 6, red line). Monitoring of the ligand exchange by UV visible measurement (right): the ultrafiltration was followed by UV spectroscopy, showing a progressive decrease of the dendron signal in the filtrate.

3. Biological effects of nanoparticles

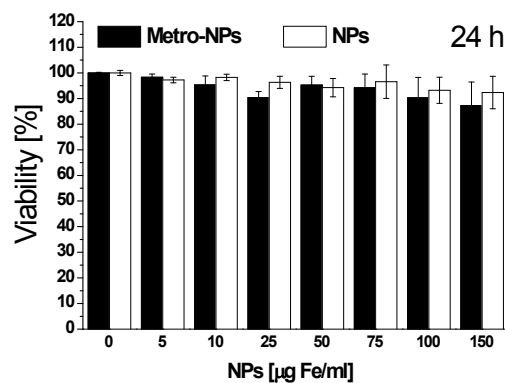
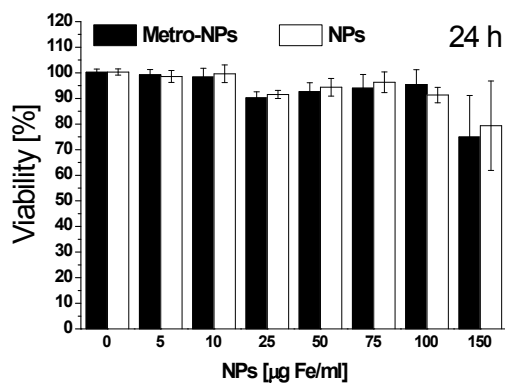
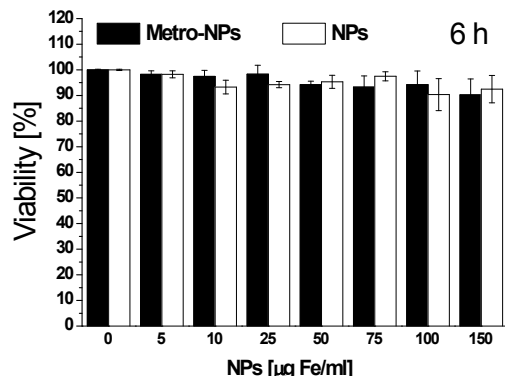
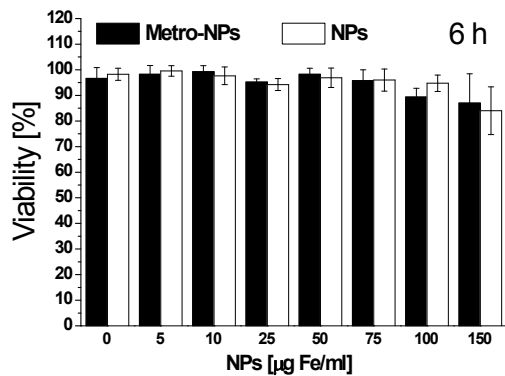
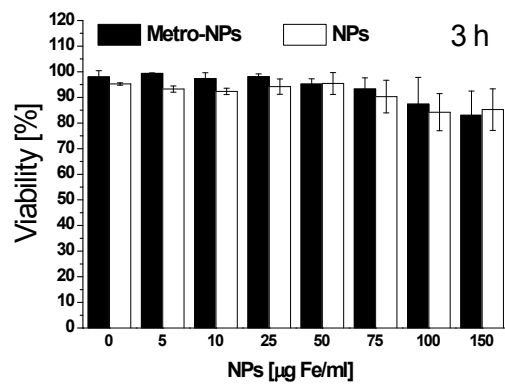
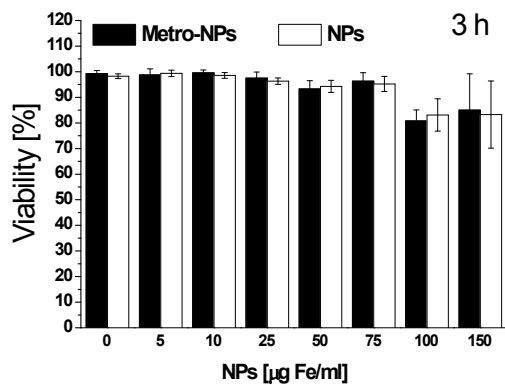
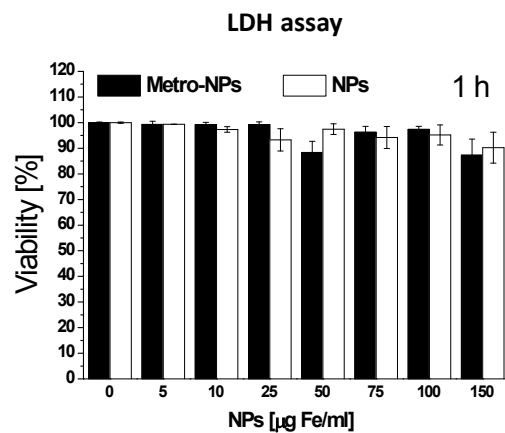
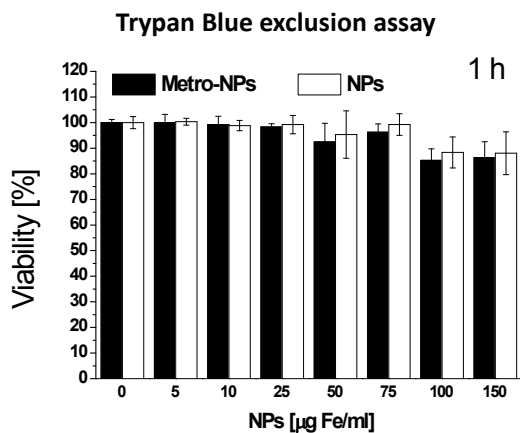


Figure S12. Effects of Metro-NPs on the viability of cells grown in monolayer. Viability of HUVEC cells after incubation (37°C) with different dosages of functionalized and unfunctionalized nanoparticles (metro-NPs and NPs) and variable time ranges, as tested by Trypan blue exclusion (left) and LDH cytotoxicity assays (right).

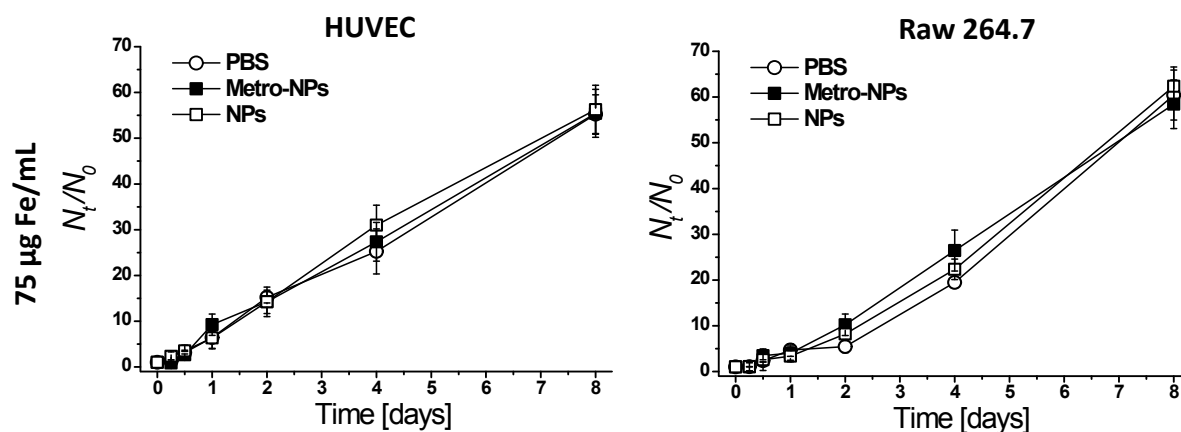


Figure S13. Effects of metro-NPs on the proliferation of cells grown in monolayer. Proliferation rates of HUVECs (left) and Raw264.7 cells (right) after incubation (37°C, 3 h) with metro-NPs and untargeted NPs (75 µg/mL). Equivalent volumes of PBS in the culture medium were used as controls.

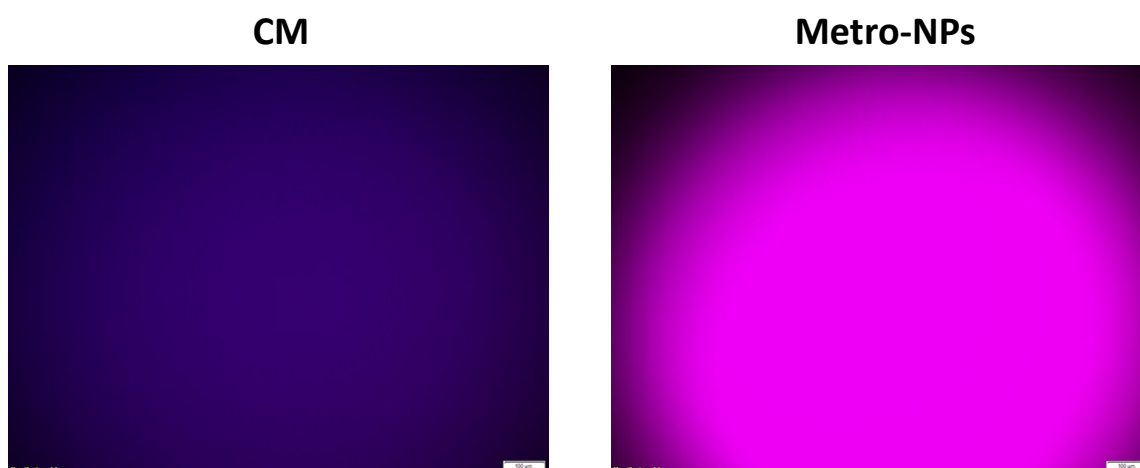


Figure S14. Fluorescence of Alexa-metro-NP. Fluorescence intensity recorded at 647 nm of the incubation medium used for the cell labeling procedure containing AlexaFluor647-decorated IONPs functionalized with metro-dendrons (IONP concentration: 25 µg Fe/ml, right). Fluorescence signal was recorded also on the control culture medium in the absence of NPs (left).

4. Hypoxia-targeting efficiency

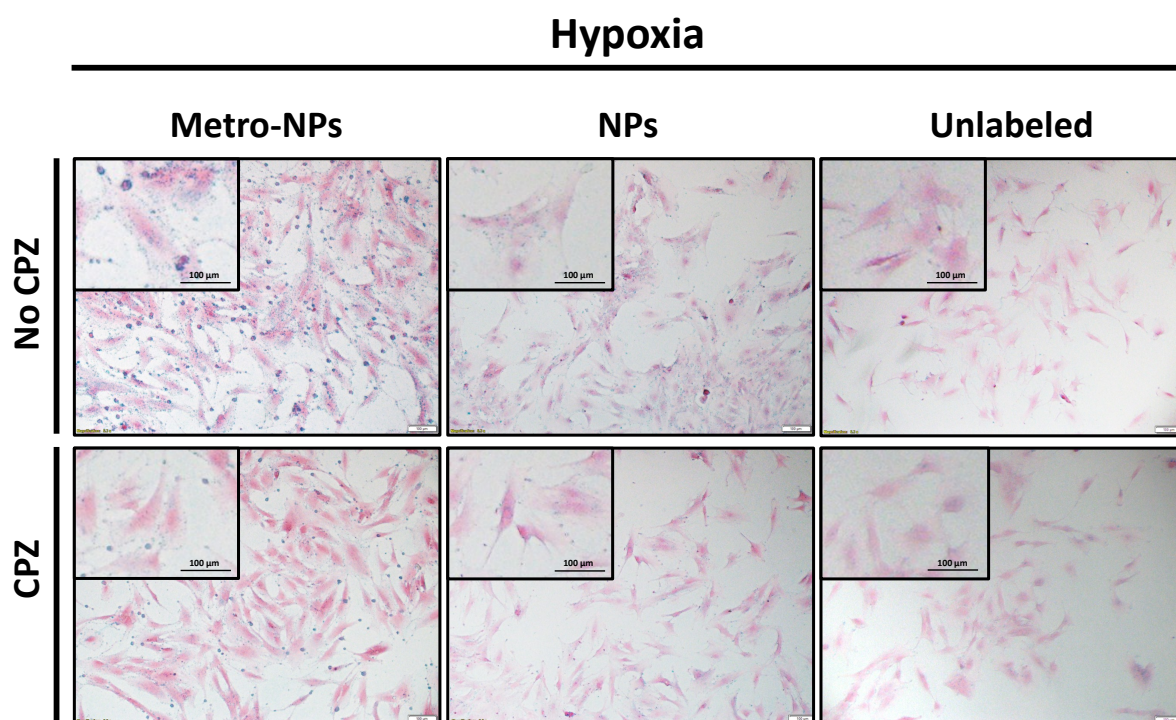


Figure S15. Internalization and retention of NPs under low oxygen tension. Prussian blue staining of HUVEC cell cultures after incubation (37°C, 3 h) with metro-NPs and untargeted NPs (25 μg/mL). Equivalent volumes of PBS in the culture medium were used as controls (unlabeled). The addition of the endocytosis-inhibitor chlorpromazine (CPZ) drastically reduced the uptake of IONPs (bottom row). The counterstaining was done for cytoplasm with eosin.

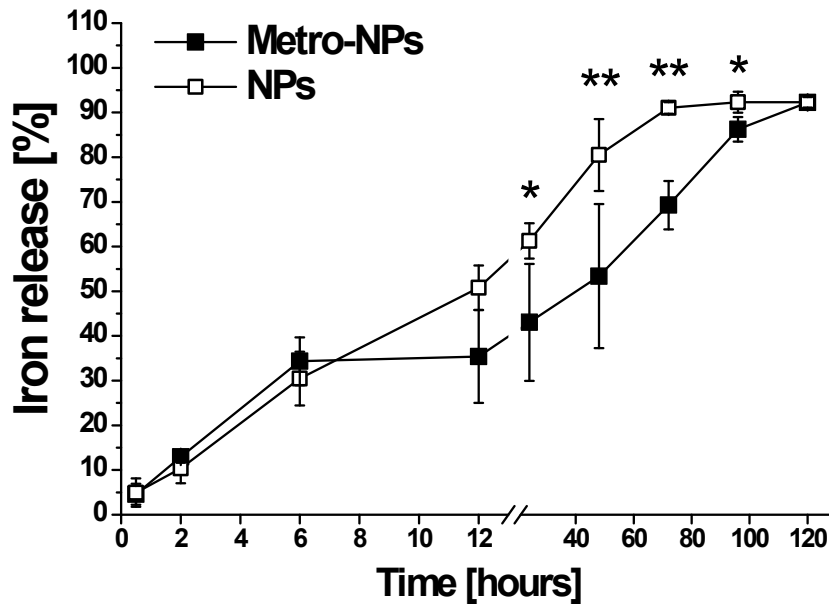


Figure S16. Release of NPs from hypoxic 3D constructs. Release of nanoparticles from constructs containing SVF cells pre-labeled with metro-NPs and control NPs (37 °C, 3 h, 25 μ g Fe/mL), expressed by quantifying the iron in the culture medium over time through absorbance measurement at 370 nm.

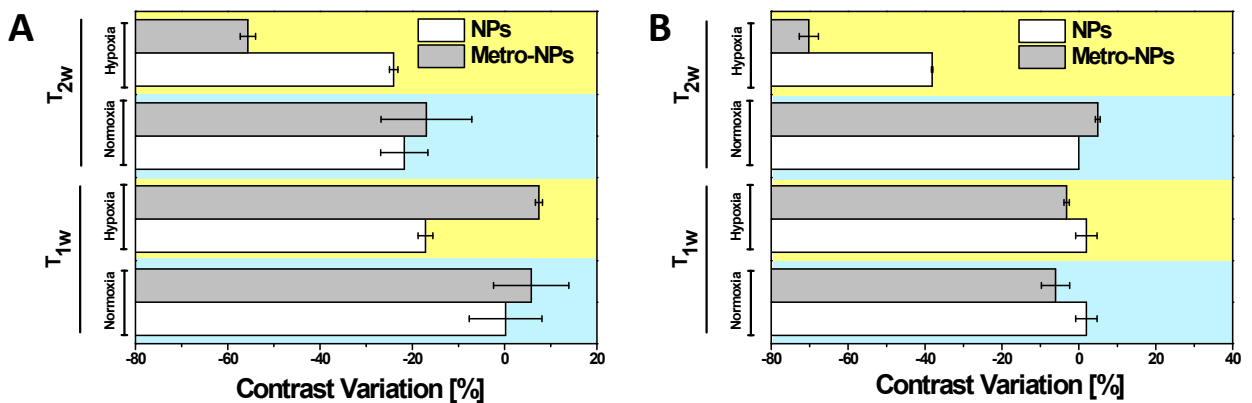


Figure S17. Contrast variation of hypoxic labeled cells in T₁/T₂ weighted imaging. Percentage Contrast Variation (CV) of labeled cell pellets with respect to unlabeled cells. The pellets of ASCs or MCF7 cells (A and B) cultured under normoxic or hypoxic conditions were subjected to T₁ and T₂-weighted imaging 3 days after incubation with PBS, NPs, and

Metro-NPs. The signal intensity was directly quantified on the images and used to calculate the percentage Contrast Variation (CV).

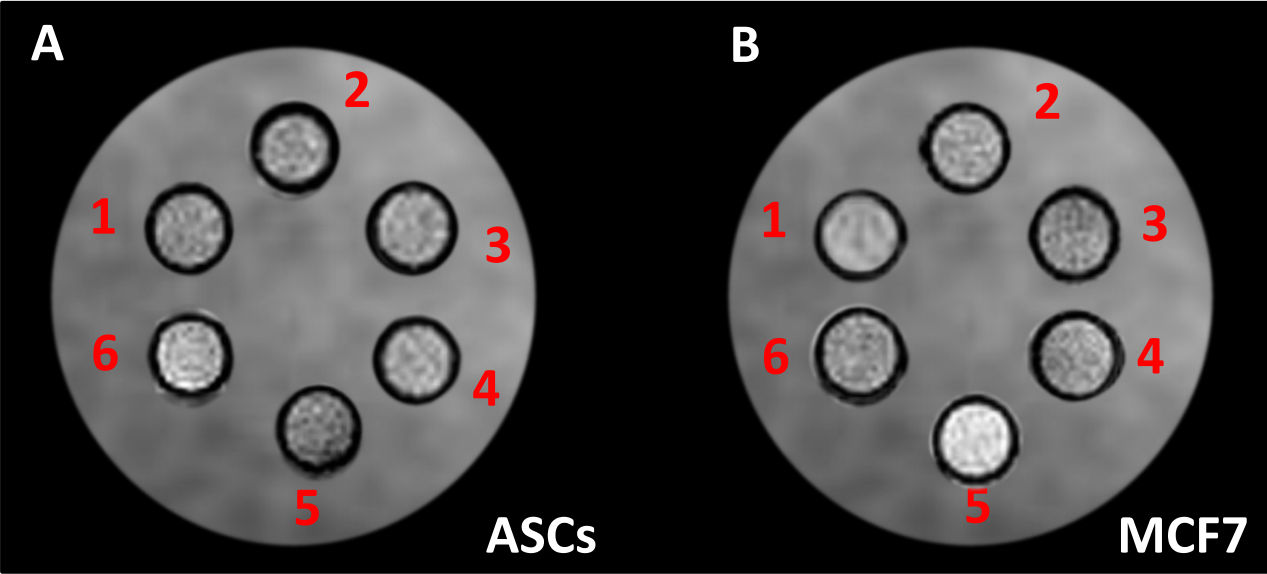


Figure S18. T_{1w} -MRI of the pellets of labeled cells. Representative T_{1w} -weighted MRI of the pellets of ASCs or MCF7 cells (A and B) 3 days after incubation with PBS (1,4), NPs (2,5), and Metro-NPs (3,6), and cultured under normoxic (1,2,3) and hypoxic conditions (4,5,6).

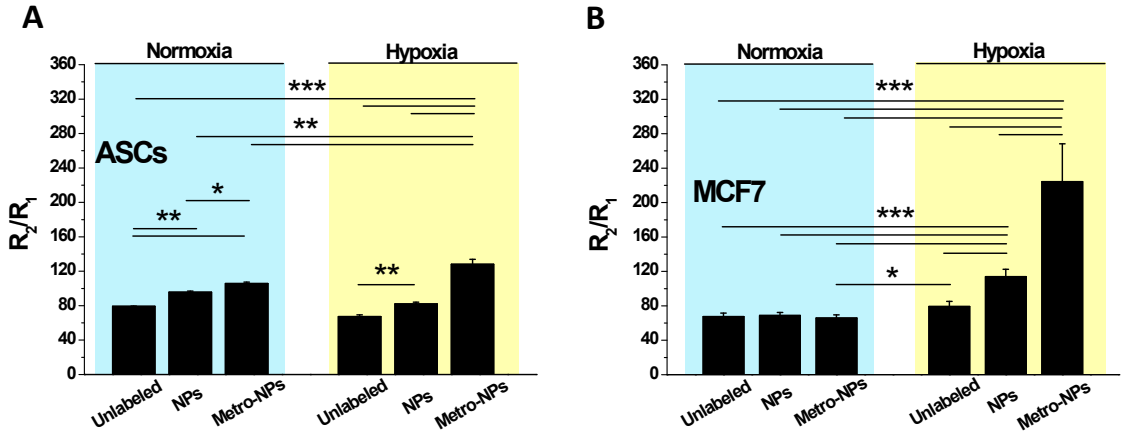


Figure S19. Relaxivity ratios of cell pellets. R_2/R_1 ratios have been calculated (Figure 7F and G) for all cell pellets, starting from relaxivity values measured by standard saturation recovery and MSME acquisition protocols. Interestingly, high ratio values were found in hypoxic ASCs and MCF7 cells labeled with metro-NPs (≈ 128 and 224 respectively).